Rate dependent load-deformation relation for concrete under impact tensile loading

J. Weerheijm[1,2]
[1]Delft University of Technology, Faculty of Civil Engineering and Geosciences, Delft 2600 GA, The Netherlands.
[2]TNO Prins Maurits Laboratory , PO Box 45, 2280 AA Rijswijk, The Netherlands

ABSTRACT

For the numerical prediction of the response of concrete structures under extreme dynamic loading reliable material data and material models are essential. TNO-Prins Maurits Laboratory and the Delft University of Technology collaborate in the field of impact dynamics and concrete modelling. The aim is to develop a (numerical) material model that covers the dynamic response of concrete up to complete failure. The first focus is on tensile loading and especially the rate effects on the failure process and fracture energy. Based on fracture mechanics and damage extension a theoretical model has been developed that describes the rate effects on the tensile strength for low and high loading rates as well. The theoretical work is combined with experiments and numerical analyses. For the loading regime up to 10 GPa/s, the gravity driven Split Hopkinson Bar of the Delft University is used. After series focusing on the tensile strength, the rate effect on the fracture energy of a single failure zone was studied. Recently, TNO-PML developed an alternative Split Hopkinson Bar test methodology which is based on the old principle of spalling. Data on dynamic tensile strength and, most important, on fracture energy at loading rates up to 1000 GPa/sec can be obtained. The first test series have been performed and confirmed the strong rate dependency of the tensile strength in the high loading rate regime (factor 5.5 at 1000 GPa/s), the fracture energy exhibits a rate dependency in this regime (upper limit of factor 2.5 at 1000 Gpa/s), while the rate dependency of the Young's modulus remains limited (factor 1.25). The test method is further developed and the possibilities to study analyse the concrete response in the experiments in detail is ongoing [1]. This paper summarizes the results of the TNO-DUT research programme. Based on the results a rate dependent softening relation is proposed.

1 INTRODUCTION AND BACKGROUND

It is well-known that the mechanical material response of concrete depends on the loading rate. Especially the tensile strength exhibits a pronounced increase beyond loading rates in the order of 10 GPa/s. Most materials exhibit a certain degree of rate dependency, but for concrete the rate dependency occurs at relatively low loading rates. The cause is the scale size of the heterogeneity [2]. Due to the composition of aggregates embedded in the mortar matrix, the dominant defects and discontinuities in concrete occur at a length scale of 10^{-3}m, while e.g. in ceramics the defects are at the scale of 10^{-6} m. For ceramics the steep strength increase in tensile strength is observed at loading rates of 10^{5} GPa/s, significantly higher than the 10 GPa/s mentioned for concrete. The rate dependency of the strength is governed by the initial damage state of the material and the contribution of the inertia effects to the extension of the (initial) damage. The damage extension has been modeled predicting the rate effect in the whole range from static loading up to loading rates of 1000 GPa/s very well. These were promising results, but for the numerical prediction of the response of concrete structures under extreme dynamic loading reliable material data and material models that include the total failure process are needed. The joint experimental and numerical research of TNO-PML and DUT focuses on the dynamic failure process. The paper outlines the current model and the experimental results. The results are combined in a rate dependent softening relation.

2 UNIAXIAL MODEL

A detailed description and background of the model is given in [2]. In summary the model is based on the following general features. (i)The tensile strength (f_t) is determined by the fracture process at micro and meso-scale. (ii) The failure process starts with bond fracture, at about 0.6 f_t, followed by matrix fracture at a load of 0.8 f_t. (iii) Beyond this level, the micro cracks in the mortar start to grow and bridging of the bond cracks occurs; macro cracks are formed; crack propagation becomes unstable and final failure occurs.

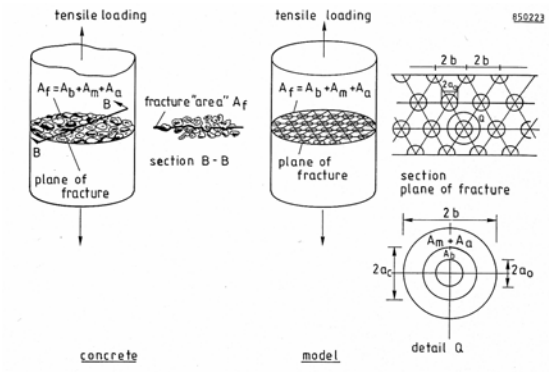

In the model the concrete is schematized as a material with penny-shaped cracks of single size 2a and at equal intermediate distance 2b. (see Figure 1). A fictitious failure plane is considered containing the flaws and representing the real failure plane. Figure 1 shows the plane of failure in concrete and the model. The initial damage is represented by cracks with radius a_o. In the model two zones are distinguished. One zone, A_b, representing bond failure and one zone, $A_m + A_a$, for mortar and aggregate fracture.

Figure 1 The fracture planes in concrete and model

The geometry of the fictitious fracture plane follows on one hand from the requirement that the dissipated fracture energy in the real material corresponds with the dissipated energy in the model. On the other hand crack extension in the fictitious fracture plane is described by using the stress- and displacement fields given by the Linear Elastic Fracture Mechanics (LEFM). Application of the strength criterion of the LEFM yields that a_o and a_c are the critical crack sizes at 0.6 f_t and 0.8f_t respectively. With these criteria the geometry of the fictitious fracture plane is defined when the strength, Young's modulus, Poisson's ratio, aggregate fraction and the specific surface energies are known. The crack extension follows from the balance of energies in the region around the crack tip. The model predicts a moderate strength increase for loading rates up to 15 GPa/s due to a changing geometry of the fracture plane.

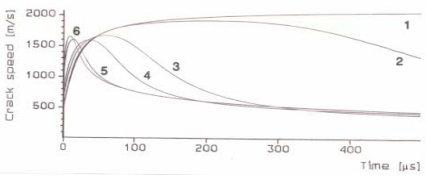

Figure 2 Crack velocity in unbounded medium

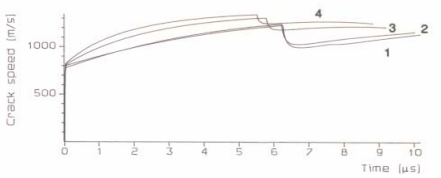

Figure 3 Crack velocity in model

Line 1-6 represent loading rates: 10^{-2}, 10^{+4},5 10^4,10^5, 5 10^5, 10^6 MPa/s

Beyond the threshold of 15 GPa/s, the internal inertia effects become dominant resulting in a steep strength increase. At the high loading rates, the singularities in the stress field vanish and the crack velocity decreases Figures 2 and 3). The model prediction of the rate dependency matches the

available data from literature very well. Based on analogous reasoning for concrete behaviour, failure development under static compression, the model was extended to the load condition of lateral static compression and axial impact loading. The predicted rate dependency as a function of the compression level is given in Figure 4.

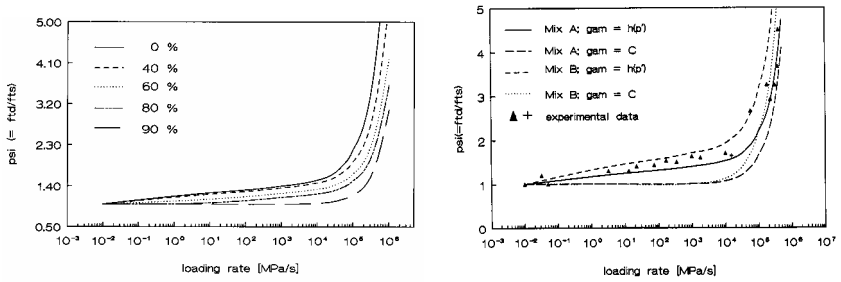

Figure 4 Rate dependency as a function of loading rate and lateral compression level(left) and the rate effect on uniaxialtensile strength with experimental data (right)

3 INSTRUMENTED SPALLING TESTS

Spalling is defined as the material failure in tension due to (partly) reflection of a pressure wave at the material transition to a material with lower acoustic impedance. TNO and DUT combine the old spall technique with up to date measurements and numerical simulations to study the concrete response at high loading rates [1]. Small detonation charges (up to 20 grams) are applied. The charge at short distance from a steel bar, loads the end of the bar and a pressure pulse propagates and impinges a concrete specimen that is situated at the opposite end of the bar. The transmitted pressure pulse reflects as a tensile pulse and failure occurs if the resulting stress exceeds the dynamic strength and the energy criterion is fulfilled. The test set-up, without the concrete specimen, is given in Figure 4, while the specimen with the location of the 8 strain gauges is given in Figure 5.

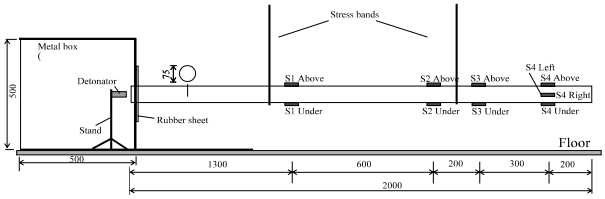

Figure 4 Schematic overview of the test set-up with the locations of the strain gauges

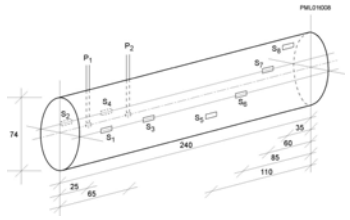

Figure 5 Instrumentation of the concrete specimen.

The development of the experimental set-up, the results and analysis of the first test series is reported in [3,4]. The incident bar and the specimen were instrumented with strain gauges recording the loading pulse, the transmitted pressure pulse to the specimen and the reflected tensile pulse. In addition the velocity of the spall debris was recorded. With the obtained data the wave propagation process was reconstructed and data on the dynamic properties of concrete could be derived. Figure 6 gives an example of strain recordings.

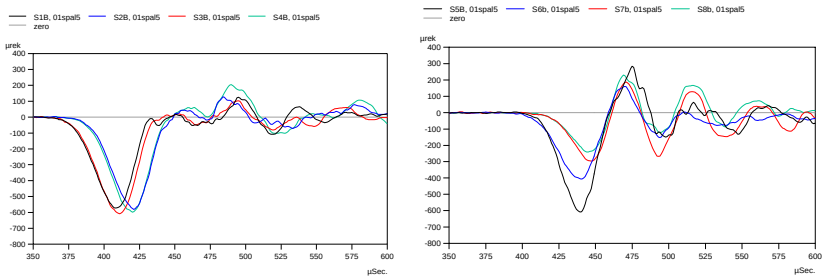

Figure 6 Strain records of the transmitted pulse at locations 1-8, test 9

To enable the study of a single failure zone, spalling tests were performed on specimen with notch depths of 0, 2 and 4 mm. The dynamic Young's modulus was derived from the recorded wave velocity. The observed rate dependency was 1,25 at the loading rate of 1000GPa/s. The dynamic tensile strength followed from the recorded reflected tensile pulse. Most reliable information about the tensile strength follows from strain record number 5 (location beyond the fracture zone) when no residual deformation is recorded. The observed rate effect is: $f_{dyn}/f_{stat} = 5.3$ at 1050 GPa/s.

From the current tests, no direct information about the fracture energy G_f is available because the deformation of the failure zone was not measured like in the previous research with the gravity driven SHB [2]. But an upper limit was obtained by considering the gross energy balance of the experiment. The terms are the compression pulse, the energy trapped in the spall debris, the (remaining) tensile pulse beyond the failure zone and the unknown fracture energy. In symbols:

$$E_{compr} = E_{debr} + E_{trans,tens} + E_{frac}$$

The material is assumed to be linear elastic except the failure zone. All energy dissipation is concentrated in the failure zone and contributes to E_{fract} ($= G_f$). The energy terms, $E_{vv} + E_{kin}$, for the stress pulses are determined using the dynamic Young's modulus value and the positive phase of the recorded pulses at the locations 1-4 and 5 for the compression and tension pulse respectively.

$$E_{vv} = \frac{1}{2} \cdot E \cdot \int \varepsilon^2(x) dl_{pulse} \quad ; \quad E_{kin} = \frac{1}{2} \cdot \int \rho \cdot v^2(x) \cdot dl_{pulse}$$

The kinetic energy of the spall debris follows from displacement measurements and the spall mass.

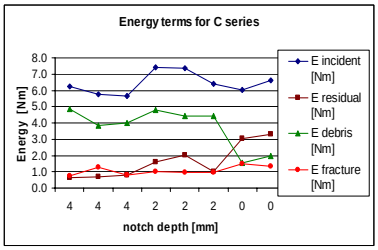

Figure 7 Energy terms of gross energy balance for the various notch depths

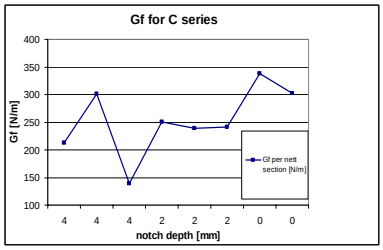

Figure 8 Fracture energy for the various notch depths

Figure 7 gives the results for the energy terms while the derived G_f values are given in Figure 8. The static G_f value for the tested concrete is about 100 J/m^2. The upper bound for the fracture

energy is $G_{f,\,dyn} < 250$ J/m^2 at loading rates of 1000 GPa/s . This result shows that the rate effect on G_f is considerably lower than for the tensile strength.

4 PROPOSED LOAD-DEFORMATION RELATION

Although the information on the dynamic fracture process is still limited, it is worthwhile to combine all the current knowledge and "define" the best possible load-deformation curve for concrete under dynamic tensile loading which can be used in numerical models. It is proposed to use the combined linear elastic ascending branch and the "Hordijk-Reinhard expression" [6] as the static reference relation. Characteristic points to judge the response and damage stage of the material are: maximum strength f_t, strain and deformation of the response zone at maximum strength (ε_{el} and δ_{el} respectively), maximum deformation of the failure zone at complete failure (δ_{frac}), fracture energy G_f. The deformation, δ, gives the elongation of the failure zone. The strain is defined as $\varepsilon = \delta / l_{frac}$. The softening curve gives the residual strength σ_{res} as a function of the non-elastic strain, ε_n. The coefficients follow from deformation controlled tests [6,7]:

$$\frac{\sigma_{res}}{f_t} = \left(1 + \left(c_1 \frac{\varepsilon_n}{\varepsilon_{frac}}\right)^3\right) \cdot \exp\left(-c_2 \frac{\varepsilon_n}{\varepsilon_{frac}}\right) - \frac{\varepsilon_n}{\varepsilon_{frac}}\left(1 + c_1^{\,3}\right) \cdot \exp(-c_2)$$

The rate effects on concrete properties depend on loading rate $\dot{\sigma}$. The "moderate regime" (< 10 GPa/s) and the "steep regime" (> 10 GPa/s) have to be distinguished. For the moderate regime the CEB relations are adopted [14].

$$\frac{f_{dyn}}{f_{stat}} = \left(\frac{\dot{\sigma}_{dyn}}{\dot{\sigma}_{stat}}\right)^{\alpha} \quad , \quad \dot{\sigma}_{stat} = 0.1 MPa/s \quad , \quad \alpha = \frac{1}{10 + 0.5 \cdot f_{c,stat}} = 0.033$$

For the rate effect on the Young's modulus the CEB proposed

$$\frac{E_{dyn}}{E_{stat}} = \left(\frac{\dot{\sigma}_{dyn}}{\dot{\sigma}_{stat}}\right)^{0.016}$$

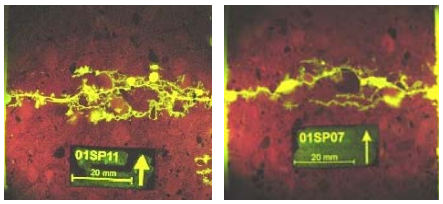

Figure 9 Examples crack pattern in spalling tests

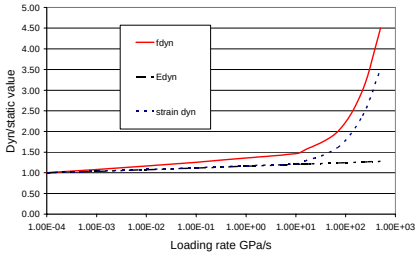

Figure 10 Rate effects for f_t, E and ε_{el}

The ratios of dynamic and static values for f_t, E and ε_{el} are given in Figure 10. The ratios beyond the loading rates of 10 GPa/s are determined by the uniaxial model (section 2) which are in accordance with the experimental strength data from literature and the new SH-tests (section 3). The instrumented spall tests showed that the rate effects on the Young's modulus does not exhibit a steep increase for loading rates up to 1000 GPa/s, therefore the CEB-formulation is applied also for the high loading rate regime.

Proposal for dynamic softening branch:

- -It is proposed to use the reference relation as derived by Hordijk for static tensile;
- -The rate effects on the tensile strength are applied (see Figure 10);

-The fracture energy G_f is constant for loading rates up to 10 GPa/s, for higher loading rates G_f increases proportional to the rate effect on tensile strength;
-The length of the fracture zone l_{frac} is constant and equals 3 Φ_{max};

Following the proposal, the softening curve can be determined consistently. For the concrete tested in the spall tests, with a static tensile strength of 3 MPa and $G_{f,stat}$ of 100 N/m, the rate dependent softening curves have been determined and depicted in Figure 11 at two amplitude scales.

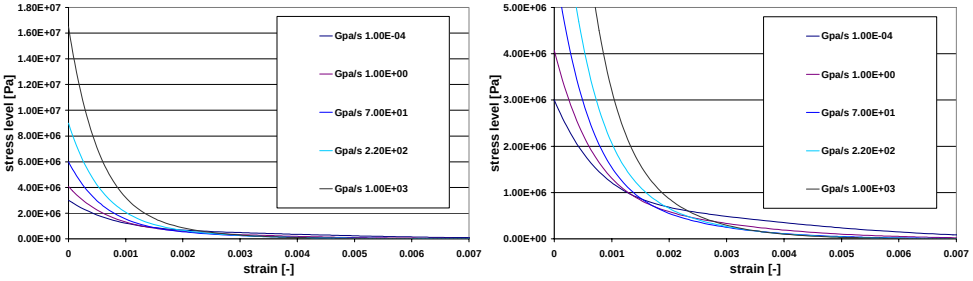

Figures 11 Dynamic softening curves at two amplitude scales.

5 CONCLUSIONS

The research to the rate effects on the failure mechanisms showed:

- A pronounced rate effect on tensile strength occurs beyond loading rates of 10 GPa/s. The rate effect has been quantified experimentally and modeled theoretically;
- The fracture energy G_f for a single failure zone is rate independent up to 10 GPa/s.
- The upper limit for the rate effect on fracture energy is 2.5 at 1000 GPa/s;
- Numerical material models and material data have to be related to single failure zones;
- A rate dependent softening relation has been derived.

6 REFERENCES

[1] R.R. Pedersen, L.J. Sluys, L.J., J. Weerheijm and A. Simone. A computational study of the fracture behaviour of concrete in a modified Split Hopkinson Bar test. 11th International Conference on Fracture, Turin, March 2005 (submitted).
[2]Weerheijm, J. Concrete under impact tensile loading and lateral compression. Doctoral thesis, Delft University, 1992.
[3]Weerheijm, J., J.C.A.M. van Doormaal and R.M. van de Kasteele. Development of a new test set-up for dynamic tensile tests on concrete under high loading rates Part 2. TNO-PML report, PML 2003-A87.
[4] J. Weerheijm and J.C.A.M van Doormaal. Tensile failure at high loading rates; Instrumented spalling tests. Int. Conf. FramCoS 5, April 2004.
[5]Concrete structures under Impact and Impulsive loading. CEB Comite Euro-International du Beton. Bulletin d' Information N° 187. August 1988
[6]D.A. Hordijk. Local approach to fatigue of concrete. Doctoral Thesis, Delft University of Technology, 1991
[7]J.G.M. van Mier. Fracture Processes of Concrete, CRC Press, Inc. 1997.